

# Simulating Thermal Conditions around Core Bolts when Transformer is Experiencing Ferroresonance

C.A. Charalambous, R. Zhang and Z.D. Wang

**Abstract--** There is a concern that the overfluxing of the core that occurs during ferroresonance can cause damage to insulation systems due to the heating of components by the eddy currents arising from the stray fields. This paper describes a case study formulated, with the purpose to quantify the thermal performance of core bolts under ferroresonance that may be present in different parts of the core. The thermal behaviour of core bolts is examined in this paper as a function of the losses. The study concludes that a core bolt depending on its location, can experience the temperature increase under ferroresonance when qualitatively benchmarking and taking the no load scenario as the base.

**Keywords:** Thermal Conditions, Core Bolts, Transformer, Ferroresonance.

## I. INTRODUCTION

Ferroresonance is attributed to the interaction between the nonlinear characteristics of transformer core and the system capacitance [1]. It is a low frequency transient or sustained phenomenon that may occur in a power transformer when one side of a double circuit transmission line connected to it is switched out [2] [3]. There is a consequent concern that the overfluxing of the core that occurs during ferroresonance can cause damage to insulation systems due to the heating of components by the eddy currents arising from the stray fields.

Overfluxing, while not enough to cause immediate failure, it could facilitate the shortening of the transformer life, especially if the system is subjected to regular ferroresonance events. It is therefore of great interest to power system owners and operators to be able to estimate the reduction in the life that could result from subjecting a transformer to sustained or transient ferroresonance. Such an interest is mainly focused on old transformers and older transformer designs, where the main limbs, yokes and any 4<sup>th</sup> and 5<sup>th</sup> limbs are held together with core tie bolts which pass through the

whole core stack by means of holes punched in each of the laminations and are insulated from the core bulk by insulating tubes of phenol paper, mica or in later units, glass fibre.

During core saturation events (e.g. Ferroresonance) the core bolt heating could be high in localized regions at the surfaces of the bolts, heat generated by the unanticipated flux flowing will be transferred to nearby insulating materials by conduction and convection, increasing the risk of accelerating insulation ageing.

This paper describes a case study formulated, with the purpose to quantify the thermal performance of core bolts that may be present in different parts of the core, under ferroresonance. The thermal behaviour of core bolts is examined in this paper as a function of the losses. Using a Finite Element method, the calculation elaborates on a micro model that is formulated using boundary conditions. The micro model contains the potential on its outer boundary interpolated from a full scale 2D transformer model at every time point.

This technique allows more detailed localized and computationally affordable thermal modelling of core bolts. Magnetic non-linearity is treated through interpolation of the transformer steel material curve and a Newton-Raphson iterative scheme to handle convergence to a solution at each time step.

Finally, a thermal transient solution by the use of global variables, which are utilised to adjust the value of the average element loss at each time step, is performed. The calculation study concludes that a core bolt can experience the temperature increase depending on its location by a qualitative benchmarking. The qualitative benchmarking is achieved by comparing ferroresonance conditions to no load conditions.

## II. CORE BOLT LOSSES

Time-domain Finite Element magnetic core modelling is able to provide visual evidence of the core state under saturating conditions such as ferroresonance and furthermore it can assess the concentrated losses caused by core bolts which may be present in older transformers. The modeling approach adopted in this paper integrates an external electrical circuit fed by balanced 3-phase voltages and a finite element transformer model, and this has been described in detail in [4].

This section describes a finite element case study formulated to quantify the losses of core bolts that may be present in different parts of the core. Specifically, it examines the difference in loss that a core bolt can experience depending on its location. Historically, at one extreme, a single bolt of large diameter was used at a small number of points on the

---

C.A. Charalambous is with the Department of Electrical and Computer Engineering of University of Cyprus, PO Box 20537, 1687, Nicosia, Cyprus. (E-mail: [cchara@ucy.ac.cy](mailto:cchara@ucy.ac.cy)). He was formerly a postdoctoral research associate of School of Electrical and Electronic Engineering at the University of Manchester UK where this piece of research work was conducted.

R. Zhang and Z.D. Wang are with the School of Electrical and Electronic Engineering at The University of Manchester, Manchester M13 9PL, UK. (E-mail: [ruizhang@postgard.manchester.ac.uk](mailto:ruizhang@postgard.manchester.ac.uk))  
(E-mail of corresponding author: [zhongdong.wang@manchester.ac.uk](mailto:zhongdong.wang@manchester.ac.uk)).

core. At the other extreme, many small-diameter bolts were used spreading throughout the core. The bolts might be stainless steel (relative permeability = 1, high electrical resistivity) or mild steel (relative permeability up to 2,500 but saturating, medium electrical resistivity). In all cases, the bolt would be electrically isolated from the core by the hole in the core laminations being of a larger diameter than the bolt and by the use of an insulating packer between the nut and the outer core lamination.

Fig. 1 illustrates the flux density distribution which corresponds to the time step that reflects the worst saturating conditions deduced by the finite element solution. Instantaneously, parts of the core achieve a flux density of 2.2 T during the ferroresonance event.

It should be noted, at this point, that the pattern presented by Fig. 1 is periodic for the case of fundamental mode sustained ferroresonance. This means that the same pattern is repeated in a 50 Hz cycle. In addition, Fig. 1 illustrates the typical possible locations of the core bolts, namely in the main limb area, the yoke area.

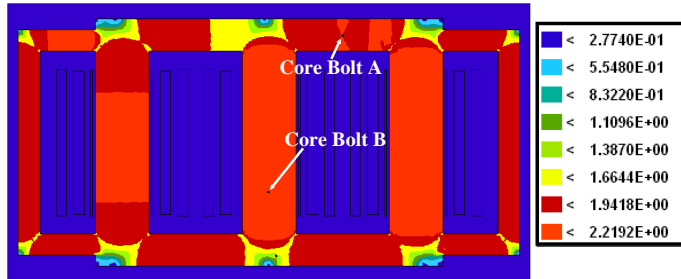


Fig. 1. Flux Density (Tesla) Distribution – Reflecting the time step of worst saturating conditions

The bolts were assumed to carry induced eddy currents which were forced to flow entirely in the component modelled in the mesh. This assumption is valid for the bolts, since they are individual components and electrically insulated from other components. Furthermore the skin effect was modelled by sub-dividing the mesh at the core bolts outer surfaces to as fine as 0.25 mm (the skin effect for steel is approximately 1mm). The discretisation of the mesh was designed to enable the elemental loss (concentrated at the outer bolt surface due to skin effect) to be modelled as accurately as possible.

Fig. 2 illustrates the flux density and flux lines distribution in the core section surrounding the bolts. It is revealed that the flux path through the bolt is concentrated to the outer surface during a core saturation condition, i.e. the flux density is the highest. The main point this illustration confirms is that when the core is saturated, the concentration of flux in the core bolts could induce eddy current heating at each side of the core bolt insulation.

The worst condition is experienced by bolt B which is located in the main limb of the core structure. The localised flux density can rise beyond 2.2 T, at the surface of bolt, even though the absolute value is dependent on the accuracy of extrapolation of the B-H curve at high flux densities, since no

measurements are currently available at these extreme conditions.

As far as bolt A is concerned which is located on the yoke area, it can be seen that even though the core has entered saturation, the core bolt is still partially screened by the core, as evidenced by the spread of flux lines around the bolt hole.

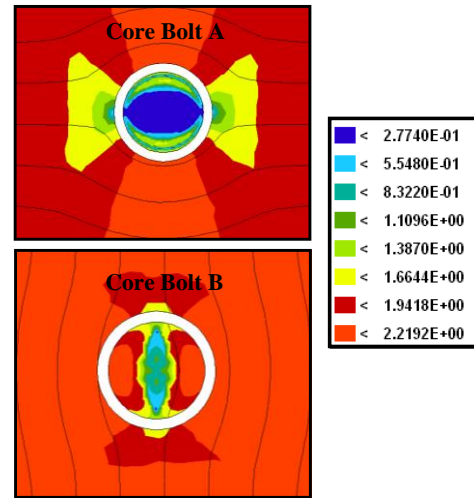


Fig. 2. Flux Density (Tesla) Distribution and Flux Lines of Core Bolts – Reflecting the Time Step of Worst Saturating Conditions.

Furthermore, by studying the sub-plots of Fig. 2 it can be concluded that the core bolt heating would be high in the localized region at the surfaces, where the flux density is higher than the rest of the core bolts.

Lastly, Figs. 3-4 illustrate the variation of the core bolt loss during the sustained mode of ferroresonance. The induced losses in core bolt (not-laminated) are the sum of the losses at each element, which is calculated using magnetic vector potential and the material properties [5]. Clearly, the losses vary very rapidly as the core swings into and out of saturation and the bolts are subjected to “bursts” of leakage flux.

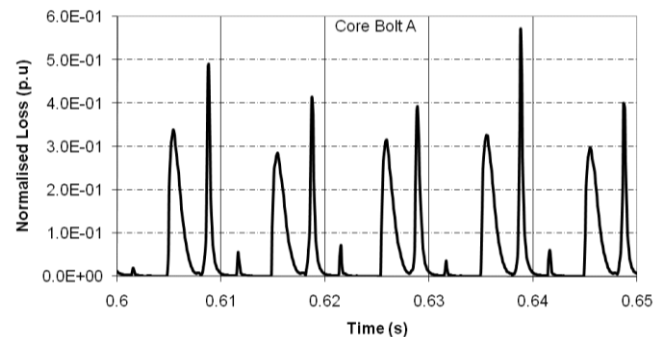


Fig. 3. Variation of Core Bolt (A) Losses with Time

Specifically, the losses were normalized by the mean loss in bolt B taken over a cycle. By comparing Figs. 3-4 it is revealed that the highest losses are encountered in core bolt B which is located on the main limb of the transformer. Under ferroresonance conditions, the phase currents are not balanced, which means that some parts of the core carry more flux than

others. This results in different degrees of saturation in different parts of the core and, thus, different losses in the bolts at different locations.

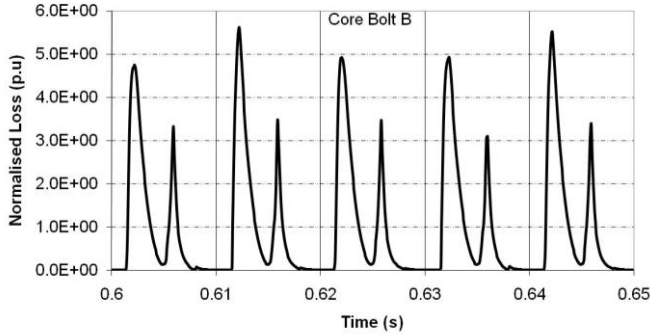


Fig. 4. Variation of Core Bolt (B) Losses with Time

As is evident from the above analysis, the location of the bolt for this particular five limb core structure will influence the severity of the losses encountered under the ferroresonance scenario. The average loss in a core bolt located at the yoke area was determined as approximately 12 times less than the loss in a core bolt at the main limb.

However, the main conclusion that is drawn is that the core bolt heating could be high in localized regions at the surfaces of the bolts therefore posing a particular danger during core saturation events. Consequently a thermal modelling endeavour becomes imperative to address the heating issue.

### III. MICRO MODEL DEVELOPMENT

The idea of creating 2-D micro-models, containing of just the bolt and the core in its immediate vicinity, pertains to the need of reducing the simulation time of a finite element transient saturation event. It is worth noting that it is computationally expensive to simulate a core model such as that of Fig. 1 which may contain core bolts at all possible locations.

Therefore, the simulation results of flux density of an entire core, having no core bolts at any possible bolt locations, are checked and the places through which the flux is the highest are identified, then the critical micro-models of these areas with bolts are formulated. Care should be taken so that the size of the micro model must be sufficiently large (i.e. its boundaries should be far enough from the bolt) that the disturbance to the core flux caused by the presence of the bolt should not be detectable at the boundary. By comparing the vector potential variation on artificial boundaries around a bolt in full size core models with and without bolts, it has been confirmed that a  $0.2m \times 0.2m$  size micro-model is sufficient for this particular ferroresonance event.

Fig. 5 details the fundamentals of the proposed micro-model approach. Fig. 6 illustrates a 2D micro model that has been created to illustrate a section of a core ( $0.2m \times 0.2m$ ) that contains a core bolt that situates in the main limb, through

which the flux is the highest.

The bolt that is modelled, in the micro model, is a standard M20 bolt which has a shank diameter of 20 mm; and a head that is 30 mm across the flats and 13 mm high. However in this particular 2-D model, illustrated by Fig. 6, projection of the head would be meaningless. Moreover, the bolt modelled has been given the non-linear B-H characteristics of mild steel BS4360. The core has been given the non-linear B-H characteristics corresponding to 27M4 laminated electrical steel. The bolts are made to be conductive and they have been given the conductivity of mild steel  $5.882 \times 10^6$  Siemens [6].

Looking at Fig. 6 the magnetic vector potential at the boundaries X and Z are positioned to account for the flux. If the bolt is located in the main limb, the flux is flowing vertically and the boundaries are also vertical. Alternatively, if the bolt is in the yoke, the flux is flowing horizontally. As a consequence the two boundaries will also be horizontal.

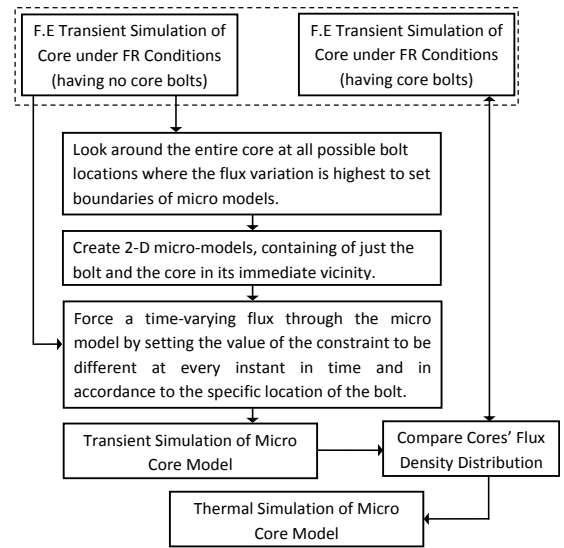


Fig. 5 Fundamentals of the micro-model Simulation Approach

The mesh of Fig. 6 was assigned time-varying boundary constraints at the two opposite edges (X and Z). The difference in the vector potential between two points (on boundary X and a corresponding on boundary Z) is the average flux density in a direction perpendicular to a straight line joining the two points. So, the different nodes on boundary X would have different potentials, therefore there is a certain amount of flux "escaping" through boundary X.

The objective is to force a time-varying flux through the model by setting the values of the constraint to be different at every instant in time. The solver interpolates the values that it requires at any particular points in time from the time varying flux data which are calculated from a transient simulation of the core (having no core bolts) under Ferroresonance.

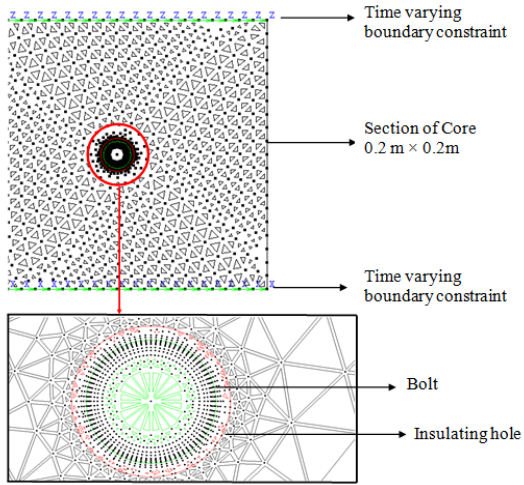


Fig. 6 Two-D Mesh Incorporating Section (with Insulated Core Bolt)

Fig. 7 illustrates the selection of two areas, one situated in the main limb area and the other situated in the yoke area on the full scale transformer core model. Fig. 8 illustrates the corresponding magnetic vector potentials at the boundaries that have been set, for the sustained ferroresonance scenario. Similarly Fig. 9 illustrates the corresponding magnetic vector potentials at the same boundaries for a no load scenario.

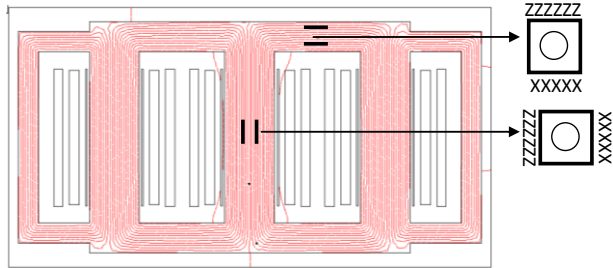


Fig. 7 Selection of Areas to Account for the Micro-Models Development

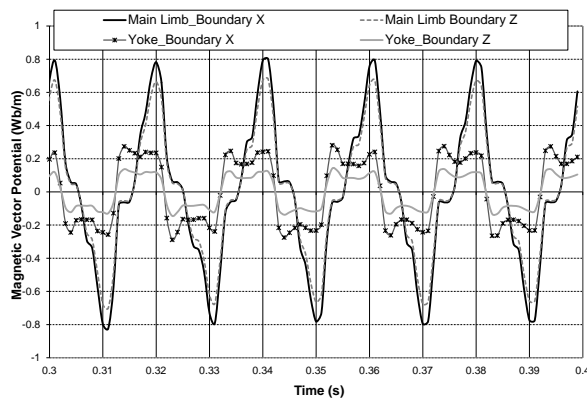


Fig. 8 Magnetic Vector Potentials at Boundaries under Ferroresonance Conditions (the difference between the vector potentials at X and Z is essentially a measure of flux)

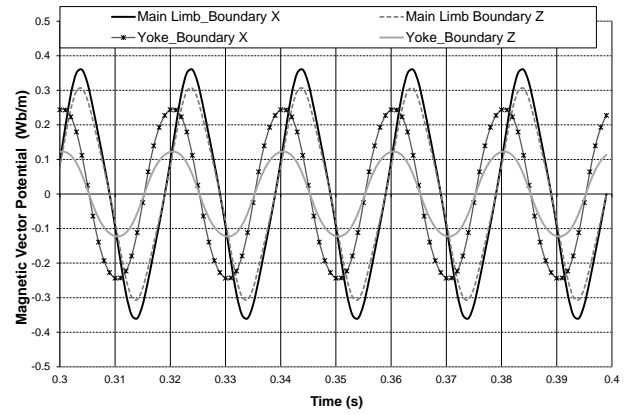


Fig. 9 Magnetic Vector Potentials at Boundaries under normal operating conditions (the difference between the vector potentials at X and Z is essentially a measure of flux)

#### IV. THERMAL MODEL

The thermal modelling has been performed by using standard available software [7]. The 2D Cartesian thermal solver employed is designed to solve the variation of temperature - throughout the nominated regions of the micro model. The solver can model directional thermal conductivities, heat capacities, fixed temperature boundaries and heat transfer surfaces. Heat sources may be specified in volumes or at surfaces [8]. Heat transfer boundaries and fixed temperature boundaries are defined by the use of line elements. The system of complex equations formed by the program is solved using the Incomplete Cholesky Conjugate Gradient (ICCG) algorithm.

Table I tabulates the nominated regions of the micro model formulated. A thermal transient solution by the use of global variables [9] utilised to adjust the value of the average element loss at each time step was then performed.

TABLE I  
THERMAL MODEL INPUT DATA

	Heat Capacity (J/kg/K)	Thermal Conductivity (Watts/m/K)
<b>Core</b>	670	48
<b>Bolt</b>	470	30.5
<b>Hole</b>	720	0.125

The thermal calculation study of the micro models was performed for two different scenarios. The first scenario concerns the bolt located in the main limb area and the second scenario concerns a bolt located in the yoke area. The micro models have been simulated under the conditions determined by the simulation of the full scale 2D transformer model (Fig. 1) for no load operating conditions and for Ferroresonance conditions. For the no load operating conditions the boundaries of the micro model have been set according to Fig. 9 while for the ferroresonance conditions the boundaries of the micro model are based on Fig. 8.

Figure 10 illustrates the fractional temperature increase that the core bolt experiences at ferroresonance when being benchmarked against the no-load conditions, both at the main

limb and the yoke area.

Figure 10 also reveals that, under the particular conditions enforced, parts of the bolt could see a temperature increase as high as 225% when located in the main limb or 113% increase, when located in the yoke area. The sections of the core surrounding the bolt located in the main limb can see a temperature as high as 162.5% whereas sections of the core surrounding the bolt in the yoke area can see a temperature as high as 109%, when core temperature produced by no-load loss is taken as baseline. It should be noted at this point that the tangible temperature reached by the core bolts and the surrounding core will be critically depended upon the cooling and this is, presently, not modelled. Furthermore, it is obvious that the temperature rise each of the core bolts experiences, would be critically depended on its relative location.

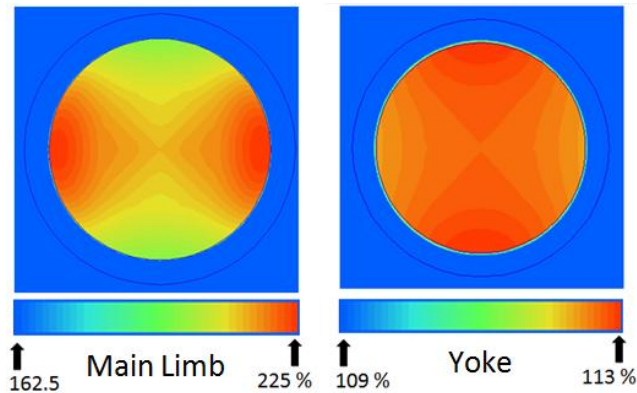


Fig. 10 Thermal Benchmarking against no load conditions

However, the outputs of the 2D thermal model presented above could be unrealistic in the sense that the bolt is being insulated by the oil around it, and (being 2D) there is no heat loss by conduction along the length of the bolt and out into the oil through the bolt head.

To overcome this, rather than doing a 3D thermal solution, another 2D thermal solution is performed on the model as illustrated by Fig. 11, which is at right angle to the one corresponding to the 2D mesh of Fig. 6.

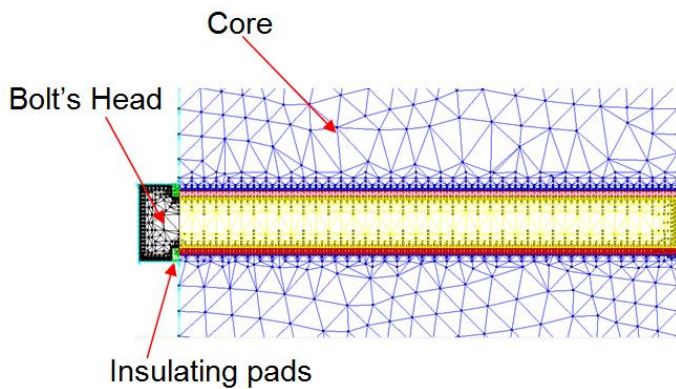


Fig. 11 Mesh Constructed for Alternative Thermal Modelling

The fundamental logic of the latter approach is that, given the fact that the heat diffuses through the bolt rapidly, it can be

assumed that the part of the bolt that is within the core has a uniform loss density. The uniform density is found by taking an area-weighted average of the values of the loss intensity (the loss in each element averaged over the last half cycle) produced by the finite element solution of the simulation model illustrated in Fig. 6. Having found that, it is used as an input value to the thermal solver that accounts for the model of Fig. 11. In this model, the bolt head is treated as a separate region with zero loss. It is therefore expected that the bolt head would draw heat out from the centre of the bolt.

Figs 12-13 illustrate the thermal outputs corresponding to the simulation of the alternative mesh of Fig. 11, for a bolt located in the main limb and a bolt located in the yoke respectively. The model has been simulated under the ferroresonance conditions. Fig 12 illustrates the thermal output where the bolt is located in the main limb.

Fig. 12 illustrates that under the simulating conditions enforced in the alternative thermal model i.e. the bolt head draws heat out from the centre of the bolt, the maximum fractional increase in temperature is found within the body of the bolt and it is as high as 200%. Fig. 12 also reveals that part of the heat is transferred to the core which exhibits a fractional temperature increase as high as 108% in the vicinity to the bolt.

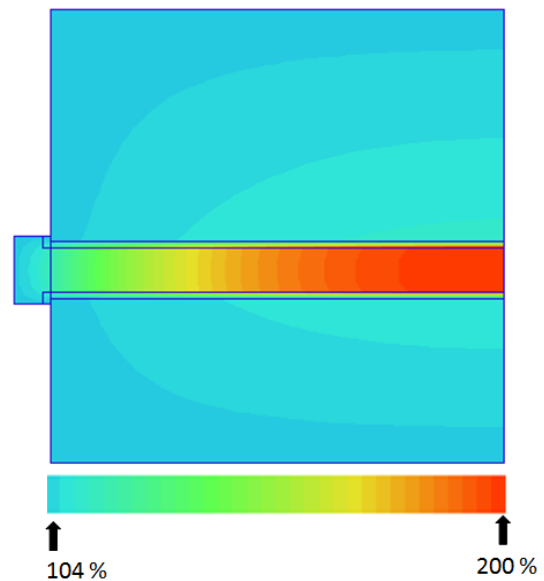


Fig. 12 Thermal Output for Bolt in the Main Limb Area

Similarly Fig. 13 illustrates the thermal output for the same simulation scenario but for the bolt located on the yoke area. 125% and 104% are the two relevant figures in terms of temperature rises at the concerned areas.

Although, the most important thermal aspect of the transformer operation is the cooling of the windings, the heat generated in other parts must not be overlooked. The simulation results of the alternative thermal model confirm that the hottest part of the core is not likely to be in a particular accessible location [10].

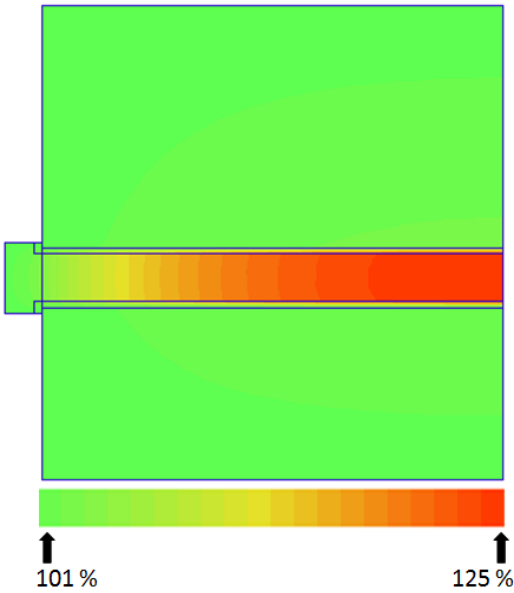


Fig. 13 Thermal Output for Bolt in the Yoke Area

The temperature of the core can only be determined by the use of thermocouples, or resistance thermometer, although the accuracy of the result would be critically dependent on the placement of the measuring device at the exact location. BS EN 60076-3:2001 [11] states that the temperature rise of the core or structural parts shall not reach temperatures which will cause damage to adjacent parts or undue ageing of the oil, acknowledging the difficulty of specifying a critical core temperature.

## V. CONCLUSIONS

The core bolt heating could be high in localized regions at the surfaces of the bolts therefore posing a particular danger during core saturation events.

Consequently, a thermal modelling endeavour becomes imperative to address the heating issue. This was achieved through the creation of 2D micro-models, containing of just the bolt and the core in its immediate vicinity to reduce the simulation time of a finite element time-domain event.

However, the outputs of the 2D thermal model presented could be unrealistic in the sense that the bolt is being insulated by the oil around it, and being 2D, there is no heat loss by conduction along the length of the bolt and out into the oil through the bolt head. To overcome this, another 2D thermal solution is performed that is at right angle to the first 2D model presented.

The study qualitatively benchmarks the temperature increase a core bolt can experience under Ferroresonance, when compared to the no load scenario. It is concluded that the bolts located in the main limb of the transformer core is most likely to exhibit large temperature increase.

## VI. ACKNOWLEDGMENT

The authors would like to express their deepest appreciation for the technical contribution of Dr. J.P Sturgess and Dr. A.

Sitzia of the SLIM Team of Alstom Grid Technology Centre towards the completion of this paper.

## VII. REFERENCES

- [1] Slow Transients Task Force of the IEEE Working Group on Modeling and Analysis of Systems Transients Using Digital Programs, "Modeling and analysis guidelines for slow transients—part III: The study of ferroresonance," *IEEE Trans. Power Delivery*, vol. 15, no. 1, pp. 255–265, Jan. 2000.
- [2] C. Charalambous, Z.D. Wang, M. Osborne, and P. Jarman, "Sensitivity studies on power transformer ferroresonance of a 400 kV double circuit," *Generation, Transmission & Distribution, IET*, vol. 2, pp. 159–166, 2008.
- [3] Rui Zhang; Swee Peng Ang; Haiyu Li and Zhongdong Wang; , "Complexity of ferroresonance phenomena: sensitivity studies from a single-phase system to three-phase reality," *High Voltage Engineering and Application (ICHVE), 2010 International Conference on* , vol., no., pp.172-175, 11-14 Oct. 2010
- [4] C. A. Charalambous, Z.D. Wang, J. P. Sturgess, P. Jarman, "Finite Element Techniques of a Power Transformer under Ferroresonance- A time domain Approach," *Submitted for IEEE Trans. Power Delivery*
- [5] Charalambous, C.A.; Wang, Z.D.; Jarman, P.; Osborne, M.; , "2-D Finite-Element Electromagnetic Analysis of an Autotransformer Experiencing Ferroresonance," *Power Delivery, IEEE Transactions on* , vol.24, no.3, pp.1275-1283, July 2009
- [6] C.A. Charalambous, Z.D. Wang, P. Jarman, M. Osborne, "Core Structure and its Association with Transformer Susceptibility towards Ferroresonance", *International Conference on Power Systems Transients (IPST2009) in Kyoto, Japan June 3-6, 2009*
- [7] SLIM version 3.9.1 ©, AREVA T&D October 2006, support.slim@areva-td.com, 2007
- [8] Slim Technical Manual for thermal models, AREVA T&D Technology Centre, Stafford, U.K., 2007
- [9] Alan Davies, "Using Global Variables Efficiently", Technical Note – Slim Technical Manual, 16 April 2004, AREVA T&D Technology Centre, Stafford, U.K.
- [10] M. Heathcote, *the J&P Transformer Book*, 12th revised edition, Elsevier Science & Technology, 1998
- [11] BS EN 60076-3:2001 "Power Transformers – Insulation Levels, Dielectric Tests and External Clearances in Air".